DISCLAIMER

This document was prepared as an account of work sponsored by the United States Government. While this document is believed to contain correct information, neither the United States Government nor any agency thereof, nor the Regents of the University of California, nor any of their employees, makes any warranty, express or implied, or assumes any legal responsibility for the accuracy, completeness, or usefulness of any information, apparatus, product, or process disclosed, or represents that its use would not infringe privately owned rights. Reference herein to any specific commercial product, process, or service by its trade name, trademark, manufacturer, or otherwise, does not necessarily constitute or imply its endorsement, recommendation, or favoring by the United States Government or any agency thereof, or the Regents of the University of California. The views and opinions of authors expressed herein do not necessarily state or reflect those of the United States Government or any agency thereof or the Regents of the University of California.

Tomographic Imaging of Water Injection and Withdrawal in PEMFC Gas Diffusion Layers

J. T. Gostick,[a] H. P. Gunterman,[b] A. Z. Weber,[c] J. S. Newman,[b] B. W. Kienitz,[c] and A. A. MacDowell.[c]

[a] Department of Chemical Engineering, McGill University, Montreal, Quebec H3A 2T5, Canada

[b] Department of Chemical Engineering, University of California, Berkeley, California, 94720, USA

[c] Lawrence Berkeley National Laboratory, Berkeley, California 94720, USA

X-ray computed tomography was used to visualize the water configurations inside gas diffusion layers for various applied capillary pressures, corresponding to both water invasion and withdrawal. A specialized sample holder was developed to allow capillary pressure control on the small-scale samples required. Tests were performed on GDL specimens with and without hydrophobic treatments.

Introduction

The behavior of liquid water in the gas diffusion layer (GDL) of polymer electrolyte membrane fuel cells (PEMFCs) has a major impact on PEMFC performance. Liquid water accumulation in the pores of the GDL blocks gas phase mass transport of reactant to the catalyst layer (CL) causing concentration polarization losses, reduces limiting current and can cause reactant starvation. Recently a number of studies have investigated

the important issue of water behavior in GDLs using water-air capillary pressure measurements (1-3). Although these methods have provided useful insight into GDL capillary properties (hysteresis, intermediate wettability, effect of hydrophobic treatment, etc.) (4) they only provide macroscopic or global information. They do not reveal any local, pore scale information about water configurations, such as the prevalence of dead end clusters, depth of water penetration, lateral spreading or residual phase distributions. For this type of detailed information it is possible to use to use x-ray computed tomography (xCT) to image the internal structure of a sample as well as water locations. xCT has been used previously to image GDL materials, but these have mostly studied dry materials (5, 6). Buchi et al. (7) have studied water injection into a GDL. They obtained images at various positive liquid pressure but did not employ capillary barriers so could not study beyond the breakthrough point or any water withdrawal. Several worker have assembled miniaturized fuel cells for studying operation, but this does not apply controlled conditions for studying only the GDL (8-11). The present work attempts to combine the macroscopic capillary pressure controlled experiments with micron resolution imaging of the GDL.

Experimental

xCT was used to image the GDL samples at different applied capillary pressures, in both the positive and negative range. The sample holder design used for traditional capillary pressure measurements required adaptation for use in the xCT setup. The main limitation was the need for the sample holder to fill but not extend beyond the field of view of the imaging system (~4 mm). An aluminum holder as shown in Figure 1 was used with a center bore hole equal to the sample diameter and a narrowed waist section

through which images were taken. Porous rods or plugs of hydrophobic and hydrophilic polymer material were inserted above and below the sample to act as capillary barriers and were held in place by a friction fit. These barriers allowed invading fluid to enter the sample and the displaced fluid to exit, without the invading fluid leaving the sample holder upon breaching the sample.

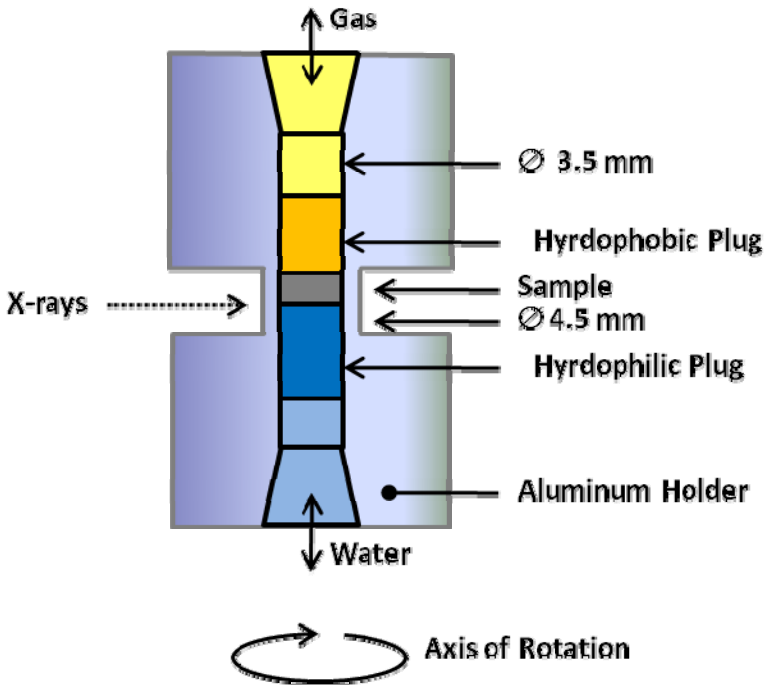

Figure 1: Schematic diagram of sample holder used to apply fixed positive or negative capillary pressure to GDLs while obtaining x-ray radiographs.

Capillary pressure was applied using hydrostatic head on the water side of the system. Due to experimental time limits it was not possible to obtain images for closely spaced capillary pressure increments. For this exploratory investigation only 5 points were measured for each sample corresponding to dry, partial water invasion, full water invasion, partial water withdrawal and full water withdrawal. Figure 2 shows the chosen

points superimposed on full capillary pressure curves of these materials that have been previously published (12). Although the capillary pressure was controlled, water saturation in the sample was not measured; however, this value can be deduced from the images.

Once the desired capillary pressure was applied 20 minutes were allowed to ensure capillary equilibrium before imaging commenced. Radiographs were taken at angular increments of 0.25° over 180° of rotation with x-ray energies of 15 keV. The number and exposure time of images was kept as low as possible to minimize damage to the sample by the radiation (9). An exposure time of 2 s per image was necessary, resulting in about 40 minutes to acquire a full set of radiographs. The imaging system was capable of resolutions of 0.9 um per pixel. Tomographic reconstructions were produced using the commercial software package Octopus. Filtering of the images prior to reconstruction was necessary to remove ring artifacts causes by defects and inconsistencies in the scintillator screen (13).

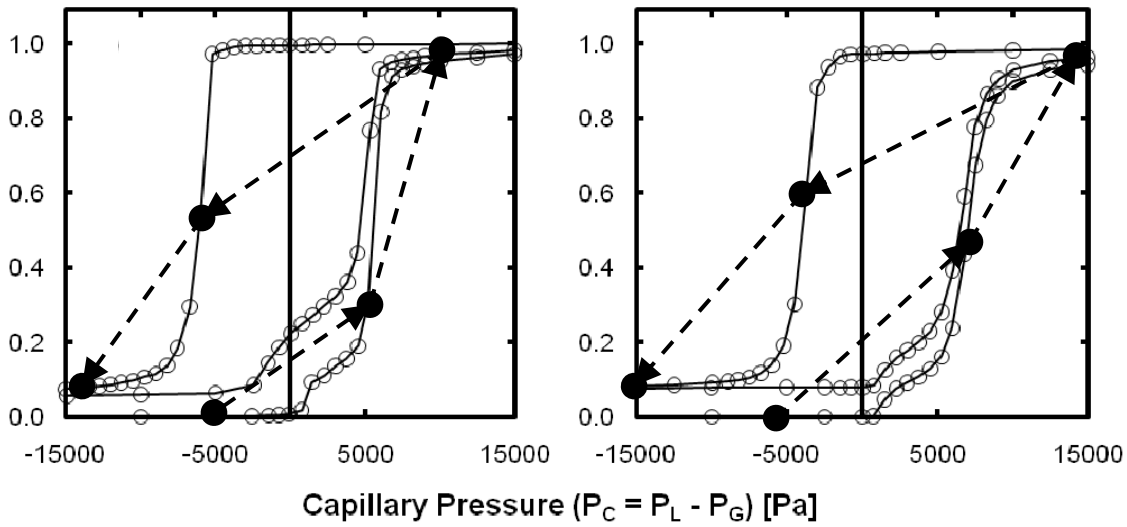

Figure 2: Capillary pressure curves for samples use in this study (Left = Toray 120A and right = Toray 120C) as reported previously (12). The points examined in the present work are denoted by the black markers which were reached along the path denoted by the dashed arrows.

Results

Tests were performed on two sets of GDLs, one with PTFE (Toray 120D) and one without PTFE treatment (Toray 120A). Slices from approximately 150, 250 and 350 microns from the injection face are shown in Figure 3 and Figure 4 for Toray 120A and 120D respectively. Each figure also shows the same slice at different applied capillary pressures and the water distribution can be observed. The images were captured at increasing then decreasing capillary pressure as shown in Figure 2 so the bottom images in Figure 3 and Figure 4 were taken first and top images last.

The grey scale values in the image correspond to the density of the phases. Darker regions are void, brighter regions are solid and intermediate values are invading water phase. Despite the observable difference in grey values between phases, each image has a mono-model histogram, making it impossible to segment these images using simple

thresholding. More advanced technique such as local thresholding and cluster/connectivity analysis would be required for further quantitative analysis.

These images do provide some qualitatively useful information however. Both samples clearly show that at the highest applied capillary pressures they are nearly completely filled but air pockets remain throughout the sample in the small crevices. This agrees the findings of macroscopic capillary pressure measure measurements where complete air displacement was observed (12). This is expected for invasion of water into a hydrophobic material where air should maintain connectivity at all water saturations (i.e. no air trapping). The images also show a small amount of residual water remaining at the most negative capillary pressure, also in agreement with macroscopic measurements.

The differences between hydrophobically treated and untreated samples is only observed in the pressure required to inject water. Macroscopic measurements do not show significant differences between residual water saturations in these two samples either. The hydrophobic coating is nearly the same density as graphite fibers so it's distribution can only be inferred from the location of thicker fibers.

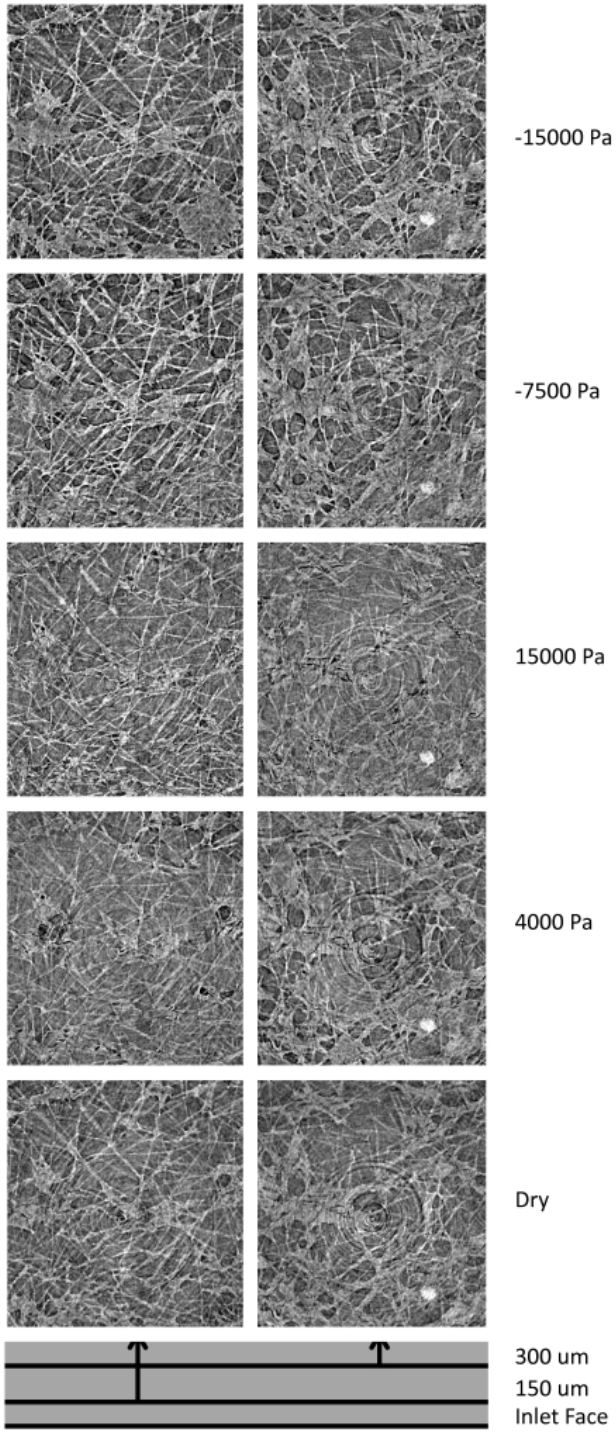

Figure 3: Reconstructed images of Toray 120A showing water configurations at different slices for successive applied capillary pressure corresponding to both water invasion and withdrawal. The white dot in the right images is an aluminum filing added fiduciary marker.

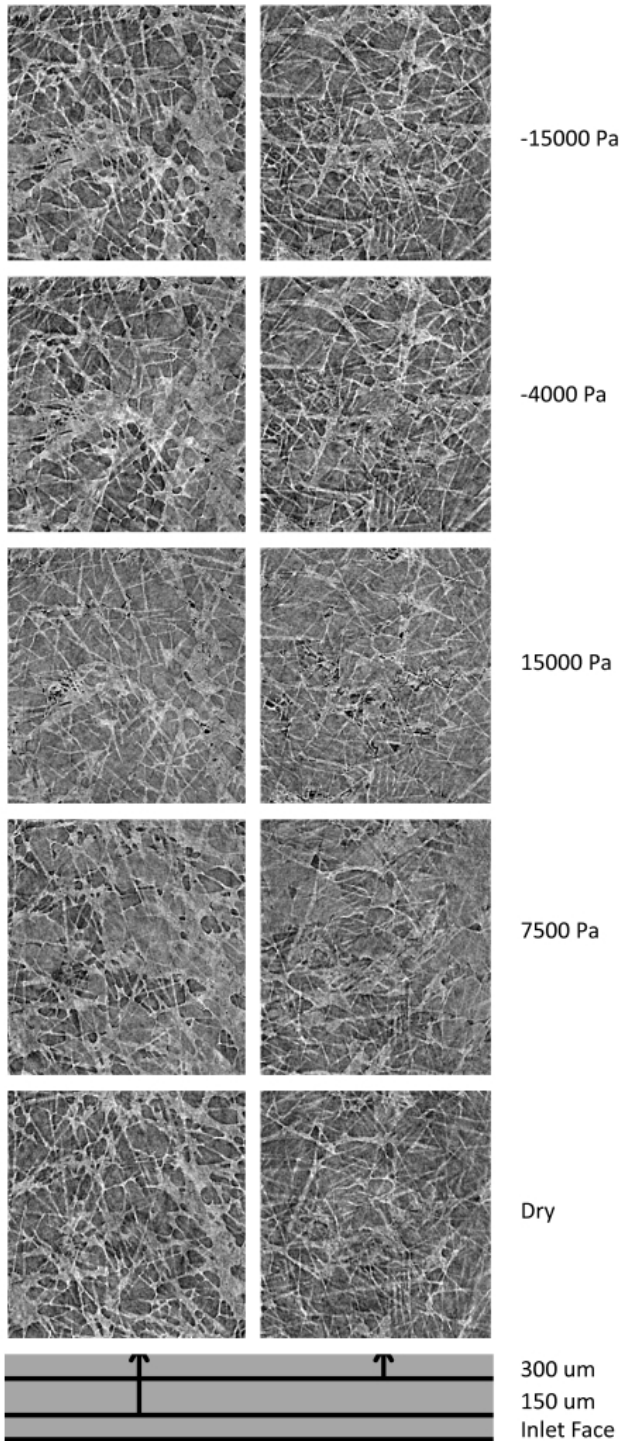

Figure 4: Reconstructed images of Toray 120D showing water configurations at different slices for successive applied capillary pressure corresponding to both water invasion and withdrawal.

Conclusions

xCT was used to visualize water configurations at various controlled capillary pressures. A sample holder was designed that allowed the application of both positive and negative pressures, enabling the scanning of complete capillary cycles and the effect of history dependence on water configuration. The grey scale values of the image show a difference between void, water and solid phases but the segmentation of the images remains a challenge.

Acknowledgments

This work was funded by the Assistant Secretary for Energy Efficiency and Renewable Energy, Office of Fuel Cell Technologies, of the U. S. Department of Energy under contract number DE-AC02-05CH11231. The Advanced Light Source is supported by the Director, Office of Science, Office of Basic Energy Sciences, of the U.S. Department of Energy under Contract No. DEAC02-05CH11231.

References

1. J. T. Gostick, M. A. Ioannidis, M. W. Fowler and M. D. Pritzker, *Electrochem. Commun.*, **10**, 1520 (2008).

2. J. D. Fairweather, P. Cheung, J. St Pierre and D. T. Schwartz, *Electrochem. Commun.*, **9**, 2340 (2007).

3. I. R. Harkness, N. Hussain, L. Smith and J. D. B. Sharman, *J. Power Sources*, **193**, 122 (2009).

4. J. T. Gostick, M. A. Ioannidis, M. W. Fowler and M. D. Pritzker, in *Modern Aspects of Electrochemistry*, C. Y. Wang and U. Pasaogullari Editors, Springer, Berlin (2010).

5. H. Ostadi, P. Rama, Y. Liu, R. Chen, X. X. Zhang and K. Jiang, *J. Membrane Sci.*, **351**, 69 (2010).

6. P. Rama, Y. Liu, R. Chen, H. Ostadi, K. Jiang, X. Zhang, R. Fisher and M. Jeschke, *J. Fuel Cell Sci. Tech.*, **7**, 031015 (2010).

7. F. N. Büchi, R. Flückiger, D. Tehlar, F. Marnoe and M. Stampanoni, *ECS Trans*, **16**, 587 (2008).

8. C. R. Wilke, *Chem. Eng. Prog.*, **46** 95 (1950).

9. A. Schneider, C. Wieser, J. Roth and L. Helfen, *J. Power Sources*, **195**, 6349.

10. C. Hartnig, I. Manke, R. Kuhn, S. Kleinau, J. Goebbels and J. Banhart, *J. Power Sources*, **188**, 468 (2009).

11. P. K. Sinha, P. Halleck and C. Y. Wang, *Electrochem. Solid-State Lett.*, **9** A344 (2006).

12. J. T. Gostick, M. A. Ioannidis, M. W. Fowler and M. D. Pritzker, *J. Power Sources*, **194**, 433 (2009).

13. B. Münch, P. Trtik, F. Marone and M. Stampanoni, *Opt. Express*, **17**, 8567 (2009).